Structure and Dynamics of Ionic Aggregates in Ethylene Ionomers and Their Effect on Polymer Dynamics: A Study by Small-Angle X-ray Scattering and Electron Spin Resonance Spectroscopy

Shoichi Kutsumizu,*,† Masahiro Goto,† Shinichi Yano,† and Shulamith Schlick‡

Department of Chemistry, Faculty of Engineering, Gifu University, 1-1 Yanagido, Gifu 501-1193, Japan, and Department of Chemistry, University of Detroit Mercy, Detroit, Michigan 48219-0900

Received December 7, 2001; Revised Manuscript Received May 7, 2002

ABSTRACT: The phase-separated morphology and the effect of ionic aggregation on the backbone chain mobility in poly(ethylene-*ran*-methacrylic acid) (EMAA) ionomers neutralized by Na^+ were investigated as a function of the degree of neutralization, *x*, by spin-probe electron spin resonance (ESR) spectroscopy and small-angle X-ray scattering (SAXS). The shape and size of the aggregates and the number of ionic groups (anions and counterions) in each aggregate were determined by SAXS, which showed that the ionic core of the aggregate is a sphere with radius of ≈6 Å that contains 7−12 ionic groups; in addition, the results strongly suggested that the sphere is covered by a shell of chain segments whose electron density is slightly lower than that of the ionomer matrix. The ESR spectra of five nitroxide spin probes differing in their hydrophilicity and in the position of the nitroxide group with respect to the headgroup were analyzed. The results indicated that the probes are position-selective and can provide information on the local polarity and mobility in, and near, the ionic aggregates. The effect of ionic aggregation on the backbone chain mobility was determined from the analysis of the ESR spectra of the spin probes at ambient temperature and in the "rigid limit" (77 K); the spectra clearly indicated the highly restricted mobility of the chain segments in the hydrocarbon shell surrounding the ionic aggregates. This study showed the complementarity of SAXS and ESR spectroscopy for deducing the phase structure and dynamics in ionomers.

Introduction

Semicrystalline ionomers are industrially important materials used in numerous applications.[1,2] A typical example is poly(ethylene-*ran*-methacrylic acid) (EMAA) partly or completely neutralized by metal cations.[3] In these materials, the incompatibility between the ionic and nonionic moieties in the system leads to the formation of a phase-separated morphology consisting of three regions: crystalline lamellae, amorphous matrix, and ionic aggregates.[4,5] These regions are interconnected, and their presence is crucial for improving polymer properties such as impact resistance, elasticity, optical clarity, melt strength, oil resistance, and adhesion.

Despite a large number of studies on the salts of EMAA ionomers, documented over more than 3 decades, a number of fundamental issues have remained unsolved, mostly due to the complexity of the ionomers and especially due to the presence of both amorphous and crystalline domains. For example, information about the size, shape, size distribution, and spatial distribution of the ionic aggregates is incomplete and often only qualitative. Recently, new experimental methods such as scanning transmission electron microscopy (STEM)[6] and atomic force microscopy (AFM)[7] have been used to resolve these issues. Both approaches have indicated that the ionic aggregates in Zn-neutralized EMAA ionomers have a spherical shape with diameter of 20−30 Å and that the size is independent of the degree of neutralization. The size of the ionic aggregates derived by these methods is however not consistent with the earlier estimates of ≈10 Å, deduced by small-angle X-ray scattering (SAXS).[8] The advantage of the two microscopic techniques compared to scattering techniques is that the structural information deduced is model independent, but the size may be slightly overestimated when the measurements are close at the resolution limit.

Information about the structure of, and near, the ionic aggregates and the molecular dynamics is also limited. The most recent comprehensive and general model of ionomers presented by Eisenberg et al. has predicted that the mobility of polymer segments surrounding the ionic aggregates ("multiplets") is greatly restricted;[9] this prediction is a key to understanding of the phase behavior and dynamics in ionomers. The first experimental support for the restricted mobility of chain segments adjacent to the multiplets has been obtained in 1994 from NMR studies of telechelic ionomers.[10]

ESR spectroscopy is an important tool for probing the local environment around species containing unpaired electrons. Early ESR studies in ionomers have analyzed ESR signals from paramagnetic transition-metal cations in an attempt to obtain the local coordination structure.[11−13] ESR spectra of nitroxide free radicals doped in ionomers as "spin probes" provided important data on the local environment and dynamics.[14−23] In the case of aqueous solutions and water-swollen membranes of Nafion[14−17] and EMAA[19−21] ionomers, ESR studies based on amphiphilic spin probes have been successful in deducing details on the local polarity and molecular dynamics around probes located in different sites in and near the ionic aggregates in the ionomers. The information obtained was consistent with and complementary to that obtained by other methods, for example using

† Gifu University.
‡ University of Detroit Mercy.
* To whom correspondence should be addressed. E-mail: kutsu@cc.gifu-u.ac.jp.

10.1021/ma012132y CCC: $22.00
Published on Web 06/27/2002

Chart 1

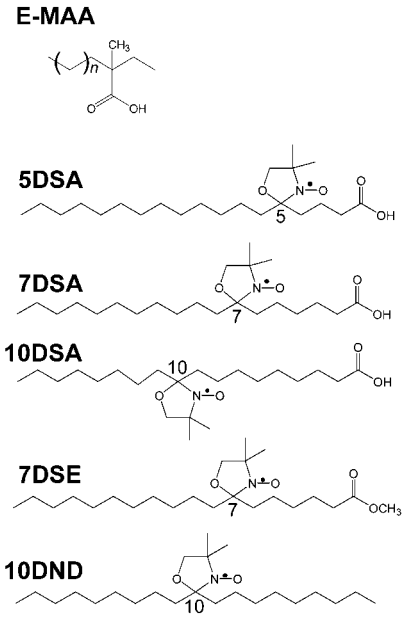

SANS[24−26] and dielectric spectroscopy.[27] ESR studies have provided additional support for the existence of a layer of polymer chains adjacent to the ionic aggregates,[18,20] as predicted in the model.[9] Very recently, a new approach using double electron−electron resonance spectroscopy was presented for the characterization of ionic aggregates,[23] and the importance of ESR spectroscopy has been growing in the field of phase-separated materials such as ionomers.

The present paper describes a study of dry EMAA ionomers using SAXS and spin probe ESR. The main objective of this study was to deduce quantitative information on the polarity and dynamics at different sites in the phase-separated system, with focus on the ionic aggregates and chains located in the vicinity of the aggregates. The results from ESR were compared with the structural information obtained from SAXS and with dynamics information obtained previously from dielectric studies of the same ionomers.

Experimental Section

Materials. The EMAA ionomers were a gift from Technical Center, Du Pont-Mitsui Polychemicals Co. Ltd., Chiba, Japan. The starting polymer, with $M_n = 19\,000$ and $M_w = 95\,000$, contained 5.4 mol % MAA units in the backbone, and the melt index (MI) was 60 g/10 min. The average number of backbone carbons between two neighboring COOH groups was therefore ≈36. The COOH groups were partially neutralized with Na, Mg, and Zn to produce ionomers denoted as EMAA-*x*Na, -*x*Mg, and -*x*Zn, respectively, where *x* is the degree of neutralization ($0 \le x \le 1$). The detailed neutralization procedure has been reported.[28] Low-density polyethylene (LDPE) was from Mitsui Chemicals Co., Ltd., Chiba, Japan, with $\rho = 0.923$ g cm^{-3}, MI = 3.7 g/10 min, $M_n = 31\,000$, and $M_w = 326\,000$.

The spin probes used in this study are illustrated in Chart 1. Four probes (5DSA, 7DSA, 10DSA, and 7DSE) are based on stearic acid, and one (10DND) has a nonadecane backbone. They differ in their polarity and/or in the position of the nitroxide group with respect to the headgroup; the number in each probe notation represents the nitroxide group position. They were purchased from Aldrich and used as received.

The spin probes were introduced in the ionomers by dipping the ionomer films into the aqueous probe solutions/dispersions of ≈0.1 mM, using the procedure described previously.[15−17,19−21] The polymer pieces were then dried in a vacuum oven at 403 K for 2 h[29] and sealed in quartz tubes under vacuum. Thus, all the samples containing the spin probes were water-free. The concentration of the spin probes in the ionomer was adjusted and low enough to avoid broadening of the lines by spin−spin interactions; the probe concentration was roughly estimated, and the ratio [COO$^-$ + COOH]/[spin probe] was 10^3−10^4.

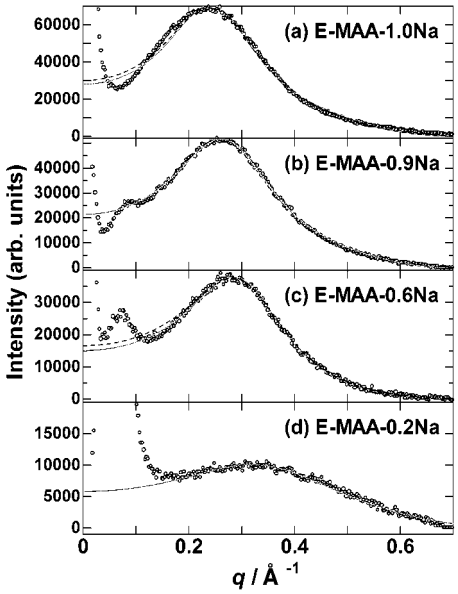

Figure 1. SAXS data for EMAA-1.0Na (a), EMAA-0.9Na (b), EMAA-0.6Na (c), and EMAA-0.2Na (d). Shown are experimental points (○) and simulations based on two liquidlike models: Yarusso−Cooper model (- - -) and depleted-zone core−shell model (——).

ESR and SAXS Measurements. ESR spectra at room temperature (293 K) were measured with the JEOL JES-TE200 X-band spectrometer equipped with the ES-DVT3 variable-temperature (VT) unit and with the Bruker ESC106 spectrometer equipped with the ER4111 VT unit at a microwave frequency of ≈9.4 GHz and 100 kHz modulation in both cases. The magnetic field was calibrated with an X-band frequency counter and Mn^{2+}/MgO, Cr^{3+}/MgO, and diphenylpicrylhydrazyl (DPPH) standards. In most cases only the separation of outer peaks in the spectra, denoted $2A'_{zz}$ in this paper, was used as a measure of the probe dynamics. The spectra at 77 K, measured in a liquid nitrogen finger dewar inserted in the cavity, directly provided the tensor component in the rigid limit, $2A_{zz}$.

SAXS measurements were carried out at the Photon Factory beamline BL-10C, the National Laboratory for High Energy Physics, Tsukuba, Japan. The synchrotron radiation with $\lambda =$ 1.488 Å and point-focusing optics were used. Details of the optics, measurements, and data treatments are described elsewhere.[30] Simulations of the SAXS curves were done both in *r*-space as well as *q*-space in the range $q = 0.15$−0.62 Å^{-1}. In *r*-space, the distance distribution function $p(r)$ was calculated on the basis of the intensity data $I(q)$ for *q* in the range 0.15−0.62 Å^{-1}, which covers the ionic peak only.

Results and Discussion

1. SAXS Results. (a) Density Profile of Ionic Aggregates. Figure 1 shows SAXS profiles of EMAA-*x*Na ionomers with $x = 0.2$, 0.6, 0.9, and 1.0, together with the best fits based on the models mentioned below. The four ionomers show a broad *ionic peak* at $q \approx 0.3$ Å^{-1} and an upturn below $q \approx 0.04$ Å^{-1}, where $q = (4\pi/\lambda)\sin\theta$, and λ (= 1.488 Å) and 2θ are the wavelength and scattering angle, respectively, of the X-rays. As with most ionomers, the peak and upturn are associated with the presence of ionic aggregates.[1,2] The upturn below *q*

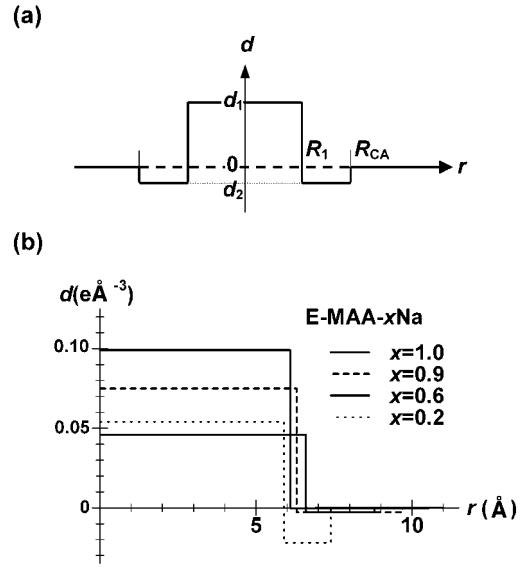

Figure 2. (a) Schematic density profile of a depleted-zone core−shell structure for the ionic aggregates, where parameters d_1 and d_2 for the electron density and R_1 and R_{CA} for the size are defined. (b) Comparison of SAXS-derived profiles for EMAA-*x*Na, with $x = 1.0$, 0.9, 0.6, and 0.2.

≈ 0.04 Å^{-1} is a result of the inhomogeneous distribution of ionic groups and/or ionic aggregates in the matrix on a length scale of 10^2 Å. A peak at $q \approx 0.07$ Å^{-1} is assigned to the stacking of polyethylene lamellae; as expected, this peak is weaker at higher degrees of neutralization, x.

The ionic peak is analyzed on the basis of the liquidlike model, which postulates that ionic aggregates in ionomers are spherical particles consisting of an ionic core of radius R_1 and a shell of hydrocarbon chains with outer radius R_{CA}; the spheres are dispersed in the amorphous matrix region with a liquidlike order under the limitation of the closest approach, $2R_{CA}$. In the original model by Yarusso and Cooper,[8] the electron density of the core is by d_1 higher than, but that of the shell is equal to, that of the surrounding matrix. As illustrated in Figure 2a, however, we postulated that the electron density of the shell is lower than that of the matrix by $|d_2|$, where $d_2 < 0$; this is the depleted-zone core−shell model. Support for this type of profile comes from the ESR results to be mentioned below. The density profile of the depleted-zone core−shell structure itself was first postulated by MacKnight et al. for EMAA−Cs ionomers,[31] but in their treatment only the *intraparticle* interference was considered (i.e., by assuming $v_p \rightarrow \infty$ in eq 1 mentioned just below).

The scattered intensity $I(q)$ for the liquidlike model of an ionic aggregate with the depleted-zone core−shell structure is given in eq 1,

$$I(q) = I_e N[v_1(d_1 - d_2)\Phi(qR_1) + v_{CA}d_2\Phi(qR_{CA})]^2/[1 + (8v_{CA}/v_p)\Phi(2qR_{CA})] \quad (1)$$

where

$$\Phi(x) = \left[\frac{3(\sin x - x\cos x)}{x^3}\right] \quad (2)$$

and I_e is the intensity scattered by a single electron under the experimental conditions, N is the number of aggregates in the scattering volume V, $v_1 = (4\pi/3)R_1^3$, $v_{CA} = (4\pi/3)R_{CA}^3$, and $v_p = V/N$ (the mean volume occupied by each aggregate). Here, the shape of the aggregates was assumed to be spherical, which is supported by the recent AFM results,[7] albeit a mismatch on the size. The solid curves in Figure 1 are best fits and reproduce the ionic peaks slightly better than the original liquidlike model ($d_2 = 0$), which is shown by the broken lines in Figure 1a,c. The fitting was performed for q in the range 0.15−0.62 Å^{-1}, which primarily contains the contribution of the ionic peak and almost no contribution of the lamellae peak.[30b] The distance distribution function $p(r)$ was also calculated on the basis of the intensity data $I(q)$ in the q range given above, and the simulated curve was compared with the experimental points. For simplicity, the distribution of the aggregate size was neglected in the model; the slight deviation of the fit from experimental data for $x = 1.0$ below $q = 0.2$ Å^{-1} may be due to the simplification.

Table 1. Structural Parameters for EMAA-*x*Na Ionomers Deduced from SAXS[a]

ionomer	R_1/Å	d_1/e Å^{-3}	R_{CA}/Å	d_2/e Å^{-3}	v_p/Å^3
EMAA-1.0Na	6.1	0.099[b]	10.7	−0.0002	17 600
EMAA-0.9Na	6.3	0.075	9.7	−0.0027	13 300
EMAA-0.6Na #1	6.4	0.051	8.4	−0.0061	6 800
EMAA-0.6Na #2	6.6	0.046	8.8	−0.0028	7 800
EMAA-0.2Na	5.9	0.054	7.4	−0.022	11 300

[a] R_1, diameter of the ionic core of the ionic aggregate; R_{CA}, diameter of the hydrocarbon shell; v_p, the mean volume occupied by one ionic aggregate. [b] Calculated from n_1(COO$^-$+COOH) and v_1 of EMAA-1.0Na (see text).

The parameters deduced from the fitting, listed in Table 1, were used to calculate the electron density profiles of the ionic aggregates, which are illustrated in Figure 2b. We note that only the relative values of d_1 and d_2 were obtained because the fitting procedure was performed on the relative intensity $I_{rel}(q)$, not on the absolute intensity $I(q)$. For EMAA-1.0Na, however, the electron density could be calculated as (33e × 1.4)/(957 Å^3) = 0.393 e/Å^3, where 11.4 is the number of COONa groups per aggregate (denoted below as n_1-(COO$^-$+COOH)) and 957 Å^3 is the volume of the ionic core (v_1) for EMAA-1.0Na. From this electron density value, the electron density of the polyethylene matrix (= 0.294 e/Å^3) was subtracted to obtain $d_1 = 0.099$ e/Å^3; in this way the proportionality factor connecting $I_{rel}(q)$ with $I(q)$ was determined. We should recall that the relative shape of the electron density profile is independent of the approximate scaling of the ordinate in Figure 2b.

Despite the approximations of the fitting procedure, especially from curve fitting in the presence of the polyethylene lamellae peak nearby, two important features of the ionic aggregates are evident from the parameters shown in Table 1: First, the radius of the ionic core, R_1, is ≈6 Å and changes only very slightly with increasing the degree of neutralization, x; the electron density, d_1, increases however with the increase of x, suggesting an increase of the number of counterions and a decrease of the inclusion of the backbone chains attached to COO$^-$/COOH groups in an aggregate, with increasing x. Second, the outer radius of the hydrocarbon shell, R_{CA}, increases, and the d_2 value approaches zero, with increasing x.

(b) Number of Ion Pairs per Aggregate. Two methods were used to estimate the number of ion pairs (COO$^-$Na$^+$/COOH) incorporated in an aggregate.[30b] The

Table 2. Characteristic Parameters for Ionic Aggregates in EMAA-*x*Na Ionomers Deduced from SAXS[a]

ionomer	n_1(COO⁻+COOH)	n_2(COO⁻+COOH)	n_2(COO⁻)	β
EMAA-1.0Na	11.4	17.0	17.0	0.7
EMAA-0.9Na	12.4	12.8	11.5	1.0
EMAA-0.6Na #1	12.9	6.6	4.0	2.0
EMAA-0.6Na #2	14.1	7.6	4.5	1.9
EMAA-0.2Na	10.2	11.0	2.2	0.9

[a] $n_1(\mathrm{COO^-+COOH}) = (4\pi R_1{}^3/3)/(84\ \text{Å}^3)$; $n_2(\mathrm{COO^-+COOH}) = mN_A\rho v_p/\mathrm{EW}$, [$m$, molar fraction of MAA comonomer units; N_A, Avogadro's number; ρ, polymer density (in g/Å^3); EW, ionomer equivalent weight per $(CH_2CH_2)_{1-m}(CH_2C(CH_3)COOH_{1-x}Na_x)_m$ unit (in g/mol)]; $n_2(\mathrm{COO^-}) = xn_2(\mathrm{COO^-+COOH})$ (x, degree of neutralization); β = fraction of side groups that are in aggregates (see text).

first method is based on the assumption that each ion pair occupies the same volume as in sodium hydrogenacetate, $NaH(CH_3COO)_2$. The volume per $Na(CH_3COO)$ group, v_0, was estimated to be ≈84 Å^3 from crystallographic data.[32] The number of ion pairs in an aggregate, n_1(COO⁻+COOH), was estimated by dividing the volume of the ionic core v_1 (= $(^4/_3)\pi R_1{}^3$) by v_0. Note that n_1(COO⁻+COOH) includes the nonneutralized COOH groups as well as the COONa groups. The second method is based on the assumption that all ionic groups in the volume v_p (v_p is the average sample volume per aggregate) are incorporated into an ionic aggregate. The number of ion pairs per aggregate, n_2(COO⁻+COOH), thus can be calculated from eq 3,

$$n_2(\mathrm{COO^-+COOH}) = mN_A\rho v_p/\mathrm{EW} \qquad (3)$$

where m is the molar fraction of MAA in the ionomer, N_A is Avogadro's number, ρ is the polymer density (g/Å^3), and EW is the ionomer equivalent weight per $(CH_2CH_2)_{1-m}(CH_2C(CH_3)COOH_{1-x}Na_x)_m$ unit (g/mol). The value of n_2(COO⁻) was calculated by multiplying n_2(COO⁻+COOH) by the degree of neutralization, x. In the second method, both n_2(COO⁻+COOH) and n_2(COO⁻) should be regarded as the upper limit values; the fraction of side groups in the aggregates, β, can also be estimated:

$$\beta = n_1(\mathrm{COO^-+COOH})/n_2(\mathrm{COO^-+COOH}) \qquad (4)$$

Table 2 lists the n_1(COO⁻+COOH), n_2(COO⁻+COOH), n_2(COO⁻), and β values estimated in this way.

The validity of these approximations was discussed in detail in our previous SAXS studies on noncrystalline EMAA ionomers.[30b] Two important conclusions can be deduced from the data presented in Table 2: An ionic aggregate contains 7−12 ion pairs in the Na salts of partly crystalline EMAA ionomers. A similar result was obtained for the Na salts of noncrystalline EMAA ionomers previously studied.[30b] The most surprising point is $\beta \approx 2$ for $x = 0.6$; the value of β should be in the range 0−1. However, it is possible that $\beta \approx 2$ suggests the inclusion of polyethylene backbone segments into the ionic core of the aggregates; the n_1(COO⁻+COOH) value based on v_1 obtained would be overestimated. The basis of this consideration comes from the fact that the d_1 value of the ionic core is increased, whereas the radius R_1 changes only slightly with increasing x, as mentioned above. This fact is also supported by the ESR results mentioned below, which indicated that the polarity index ΔA_0 of a spin probe inside the ionic core

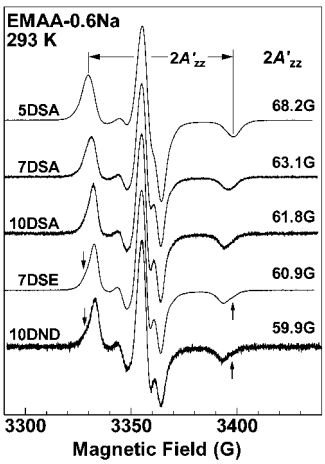

Figure 3. X-band ESR spectra at 293 K for the indicated spin probes in EMAA-0.6Na. Spectra are normalized to a common microwave frequency (9.43 GHz). Microwave power, 1 mW; modulation amplitude, 1 G. The corresponding extreme separation $2A'_{zz}$ is shown on the right. Downward and upward arrows point to the incipient shoulders in the low-field and high-field signals, respectively, for 7DSE and 10DND; these shoulders are more pronounced for EMAA-0.8Na (Figure 4).

increases almost linearly with x (Figure 8). Thus, it is reasonable to propose that $\beta \approx 2$ does not show the failure of our SAXS interpretation but reflects an interesting feature of the ionic aggregates in EMAA-*x*Na ionomers.

2. ESR Results. (a) Location of Probes. Figure 3 presents X-band ESR spectra at 293 K of four doxylstearic probes (5DSA, 7DSA, 10DSA, and 7DSE) and of 10DND in EMAA-0.6Na. The spectra extend over a broad range, from 3320 to 3410 G (1 G = 0.1 mT). Similar spectra were obtained in all the EMAA-*x*Na ionomers (x in the range 0−0.9) examined. The spectra indicate that the motional state of the probes in the ionomer is highly restricted even at 293 K. In such situations the extreme separation of outer peaks, $2A'_{zz}$, reflects the probe immobilization by the polymer and can be used as a quantitative indicator of the molecular motion. For EMAA-0.6Na (Figure 3), the $2A'_{zz}$ values are 68.2, 63.1, 61.8, 60.9, and 59.9 G for 5DSA, 7DSA, 10DSA, 7DSE, and 10DND, respectively. Since the probes have similar magnetic parameters in the same environment, the wide range of $2A'_{zz}$ values obtained suggests that the probes are located in different sites in the ionomer and report on their local environments.

Figure 4 shows the ESR spectra at 293 K of the probes in EMAA-0.8Na. The $2A'_{zz}$ values for the *n*DSA probes (with n = 5, 7, and 10) are larger than for EMAA-0.6Na, especially for 7DSA, where the $2A'_{zz}$ changes from 63.1 G for $x = 0.6$ to 67.3 G for $x = 0.8$. An additional, and remarkable, feature is seen for 7DSE and 10DND: the extreme peaks, at 3330 and 3390 G, have an additional shoulder, which is indicated by arrows in Figure 4. The splitting indicates the presence of *two* spectral components differing in their $2A'_{zz}$ values, which are shown as s_1 and s_2 in Figure 4. A similar result was obtained for 7DSE and 10DND in EMAA-0.9Na. The splitting is also detected in EMAA-0.6Na (Figure 3), although not as clearly as for the higher x values.

Two factors, local dynamics and local polarity, affect the value of $2A'_{zz}$. To separate these two effects, we determined the extreme separation in the rigid limit, $2A_{zz}$, at 77 K; at this temperature the molecular motions of the probes are frozen, and the extreme separation

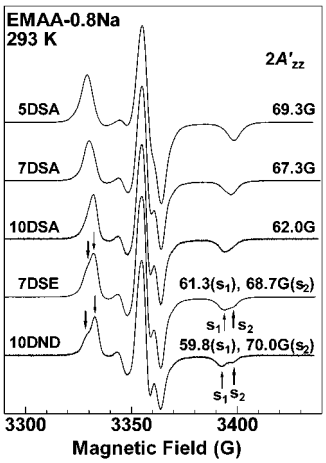

Figure 4. X-band ESR spectra at 293 K for the indicated spin probes in EMAA-0.8Na. Spectra are normalized to a common microwave frequency (9.43 GHz). Microwave power, 1 mW; modulation amplitude, 1 G. The extreme separation $2A'_{zz}$ is shown on the right. Thin and thick arrows point to the s_1 and s_2 spectral components for 7DSE and for 10DND (see text).

reflects only the local polarity.[33] Table 3 summarizes the $2A'_{zz}$ at 293 K and $2A_{zz}$ values at 77 K for all probes as a function of x, together with the data for low-density polyethylene (LDPE) for comparison; all values were measured within an uncertainty of ±0.3 G. For EMAA-0.6Na, the $2A_{zz}$ values are 69.4, 67.6, 66.7, 67.1, and 67.2 G for 5DSA, 7DSA, 10DSA, 7DSE, and 10DND, respectively. The trend is $2A_{zz}$(5DSA) > $2A_{zz}$(7DSA) > $2A_{zz}$(10DSA) < $2A_{zz}$(7DSE) ≈ $2A_{zz}$(10DND). The differences in the $2A_{zz}$ values between 10DSA, 7DSE, and 10DND are small, but the fact that the $2A_{zz}$ for 10DSA is the lowest among the three is the same for all x between 0.4 and 0.9. Therefore, this trend is considered to reflect the polarity difference between the locations of the five probes and to provide local information on the microphase separation in and near the ionic aggregates.

It is reasonable to expect that the carboxylic groups of the three hydrophilic *n*DSA probes, with $n = 5$, 7 and 10, are located in the ionic core of the ionic aggregate; the nitroxide groups of the three *n*DSA are expected to act as "spin labels" located at different distances, r, from the center of the aggregate. These distances were estimated to be 6.6, 9.8, and 12.4 Å for 5DSA, 7DSA, and 10DSA, respectively, on the basis of the Chem3D software. Figure 5 summarizes the $2A'_{zz}$ values of five probes in the EMAA-*x*Na ionomers at 293 K, together with the data for LDPE as a reference. The effect of x on the $2A'_{zz}$ values is most evident for 5DSA and for 7DSA, and the $2A'_{zz}$ values of those probes increase with increasing x. These two probes are the most hydrophilic, and the above trend is considered to reflect mainly the increased ability of the aggregate to restrict the motions of the chain segments around them with the increase of x. The two hydrophobic probes, 7DSE and 10DND, are expected to be excluded from both the ionic aggregates and the polyethylene lamellae regions and to act as "spin labels" for the hydrophobic amorphous region. In this case, however, the distance from the center of the aggregate cannot be specified. Therefore, in Figure 5 these probes are placed outside the ionic aggregates, in the amorphous matrix region. For x = 0.8 and 0.9, two $2A'_{zz}$ values are plotted for each x, as mentioned earlier.

To visualize the extent of microphase separation, we calculated the polarity index, ΔA_0 (in G): ΔA_0 (G) = A_0(ion) − A_0(np), where A_0(ion) is the isotropic ^{14}N splitting constant of the probes in the ionomer and A_0(np) is the corresponding value in a nonpolar medium, which was taken as 13.9 G for *n*DSA probes.[19,33] As seen from this definition, a larger value of ΔA_0 means a higher local polarity. Since A_0(ion) values for the probes cannot be measured directly, we estimated them using the correlation diagram between A_0 and A_{zz} for various solvents given in the literature,[33] where A_{zz} is half the extreme separation of outer peaks in the rigid limit at 77 K.

Figure 6 presents the polarity profiles based on the polarity index for the EMAA-*x*Na ionomers. As in Figure 5, the points for the hydrophilic probes were plotted as a function of r, and the points corresponding to the hydrophobic probes, 7DSE and 10DND, were placed outside the ionic aggregates, in the matrix region. Figure 6 reveals several interesting features of the microphase separation in the EMAA-*x*Na ionomers.

(1) For a given degree of neutralization, x, the polarity indices are ΔA_0(5DSA) > ΔA_0(7DSA) > ΔA_0(10DSA), in line with the values of r. This is reasonable, because a smaller r corresponds to a location deeper inside the ionic aggregate.

(2) For 5DSA and 7DSA, the ΔA_0 value increases with increasing x. This result can be taken as an indication that the higher degree of neutralization promotes the formation of ionic aggregates and is in agreement with SAXS results: as shown in Figure 2b, the electron density d_1 of the ionic core increases with x.

(3) In contrast with the behavior of 5DSA and 7DSA, the ΔA_0 value for 10DSA slightly decreased with an increase of x from $x = 0.2$ to 0.9, and the value for $x = 0.9$ is very close to the value for LDPE (0.59). In addition, for all x values (except $x = 0$) the ΔA_0 value of hydrophilic 10DSA is slightly but clearly smaller than the ΔA_0 values of hydrophobic probes 7DSE and 10DND. This indicates that the nitroxide group of 10DSA is located in a region where almost all the ionic groups are *excluded*, a region where only polyethylene segments are left. Moreover, the lowest ΔA_0 value corresponds to $x = 0.9$, indicating that the ion exclusion in the region near the ionic aggregates is most pronounced at the highest degree of neutralization.

(4) For the hydrophobic probes 7DSE and 10DND, the ΔA_0 values are ≈0.75. These values are lower than those of the hydrophilic 5DSA and 7DSA probes when $x \geq 0.4$ but larger than those of the same probes intercalated into LDPE (0.59). This fact is considered to reflect the presence of a small amount of isolated ionic groups dispersed in the amorphous region.

The results mentioned above suggest the locations of the probes and the structure of the ionic aggregates in the EMAA-*x*Na ionomers presented in Figure 7. The description of the spherical ionic aggregates consisting of an ionic core of radius R_1 and a shell of hydrocarbon chains with outer radius R_{CA} is based on the Yarusso−Cooper liquidlike model. The nitroxide group of 5DSA is located at $r = 6.6$ Å inside the ionic core, and that of 7DSA is placed at $r = 9.8$ Å at the core periphery. The nitroxide group of 10DSA is at $r = 12.4$ Å in the hydrocarbon shell. Therefore, 9.8 Å < R_1 < 12.4 Å < R_{CA}. From the SAXS results mentioned above, R_1 is ≈6 Å, almost independent of x, and R_{CA} is in the range 7.4−10.7 Å. The R_1 and R_{CA} values derived from ESR are

Table 3. Extreme Separation ($2A'_{zz}$ at 293 K and $2A_{zz}$ at 77 K) of Spin Probes in EMAA Ionomers[a]

	$2A'_{zz}$ at 293 K					$2A_{zz}$ at 77 K				
sample	5DSA	7DSA	10DSA	7DSE	10DND	5DSA	7DSA	10DSA	7DSE	10DND
EMAA-*x*Na										
$x = 0.9$	69.8	67.7	63.2	61.9 (s_1) 69.1 (s_2)	59.2 (s_1) 68.8 (s_2)	71.6	69.7	66.6	67.9	67.6
$x = 0.8$	69.3	67.3	62.0	61.3 (s_1) 68.7 (s_2)	59.8 (s_1) 70.0 (s_2)	71.1	68.9	66.8	67.6	67.6
$x = 0.6$	68.2	63.1	61.8	60.9	59.9	69.4	67.6	66.7	67.1	67.2
$x = 0.4$	65.6	62.1	60.7	61.0	60.3	68.3	67.5	66.9	67.2	67.4
$x = 0.2$	64.3	60.6	61.3	61.8	60.5	67.3	67.1	66.9	67.5	67.3
EMAA	62.7	60.9	61.6	61.7	61.7	67.0	66.5	67.4	67.3	67.4
LDPE	57.9	58.0	57.9	57.8	57.6	66.3	66.3	66.4	66.4	66.4

[a] The experimental uncertainty in the determination of those values is $\leq \pm 0.3$ G. [b] s_1, s_2, are the $2A'_{zz}$ values corresponding to two components (see Figure 4 and the caption).

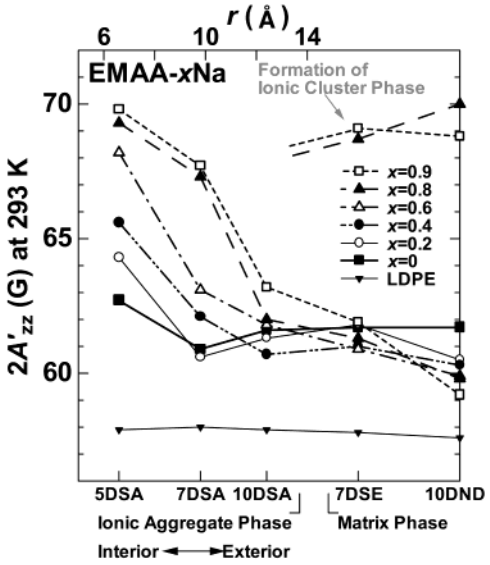

Figure 5. Variation of $2A'_{zz}$ values at 293 K for the five spin probes in EMAA-*x*Na (*x* in the range 0−0.9) with the distance from the center of the ionic aggregate, *r*, together with the data for LDPE. The *r* values were assumed identical to the distance of the nitroxide group from the carboxylic group in the *n*DSA probes (see text).

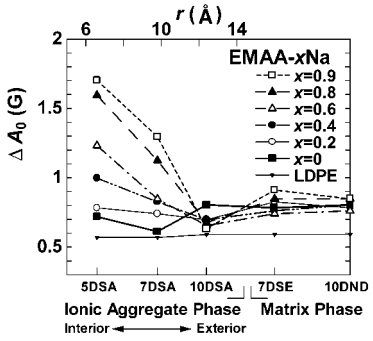

Figure 6. Variation of the polarity index ΔA_0 for the five spin probes in EMAA-*x*Na (*x* in the range 0−0.9) with the distance from the center of the ionic aggregate, *r*, together with the data for LDPE. The *r* values were assumed identical to the distance of the nitroxide group from the carboxylic group in the *n*DSA probes (see text).

larger than those deduced from SAXS; however, the agreement between the two sets of values is fairly good, considering the use of completely different techniques. We can conclude that both ESR and SAXS provide evidence for the presence of ionic aggregates with dimensions on the order of 10 Å in EMAA-*x*Na ionomers.

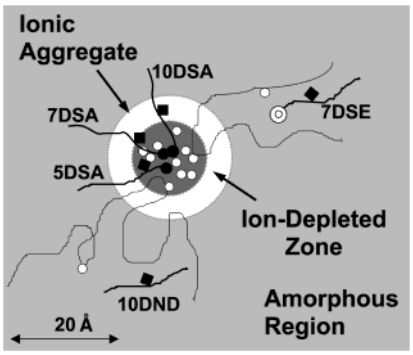

Figure 7. Suggested locations of 5DSA, 7DSA, 10DSA, 7DSE, and 10DND probes in dry EMAA ionomers, based on the analysis of the ESR results; the carboxylate and carboxylic acid groups of the ionomer (○), and the acid groups (●), the methyl ester group (◎), and the nitroxide groups (■) of the probes are indicated. Dark shaded, white, and gray-shaded regions represent respectively the ionic core and hydrocarbon shell (ion-depleted zone) of the aggregate and the amorphous region.

The fact that the local polarity at the 10DSA site is slightly lower compared with 7DSE and 10DND suggests that the shell of radius *r*, with $R_1 < r < R_{CA}$, is an *ion-depleted zone*; this is the reason for adopting the depleted-zone core−shell structure as a modification of the Yarusso−Cooper model when simulating the SAXS ionic peaks. The locations of 7DSE and 10DND in the amorphous region are also supported by the temperature variations of $2A'_{zz}$, which will be reported in the future. Consequently, the present ESR results of EMAA-*x*Na ionomers demonstrated that the five spin probes, three hydrophilic *n*DSA probes and two hydrophobic probes, are position-selective and provide local information from different sites in the ionomers.

(b) Comparison with Dielectric Studies. Dielectric relaxation (DR) can be used to study the molecular motions in polymers, through the orientation of dipoles under alternating electric field. In our DR studies of EMAA-*x*Na ionomers[34] we have detected for $x \leq 0.2$ two relaxations, near 190 and 320 K at a frequency of 1 kHz, both from the amorphous region. The low-temperature relaxation, γ, was assigned to a local molecular motion of short segments; the high-temperature relaxation, β', was assigned to a thermally activated (above T_g) micro-Brownian motion of long chain segments. For $x = 0$, the β' relaxational peak was observed at 315 K at 1 kHz, which shifted to 326 K for $x = 0.2$. Thus, the ionomers were considered to consist of two phases, crystalline and amorphous polyethylene phases, and the ionic aggregates formed for $x \leq 0.2$ were thought to be dispersed in the amorphous regions. For $x \geq 0.4$, the β' relaxation is replaced with two relaxations, β at 282−294 K and α

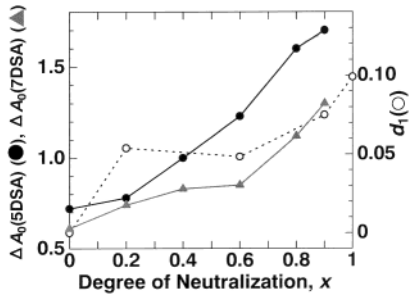

Figure 8. Comparison of the polarity index (ΔA_0) deduced by ESR and the electron density of the ionic core (d_1) deduced by SAXS: Plots of ΔA_0 values for 5DSA [ΔA_0(5DSA)] and for 7DSA [ΔA_0(7DSA)], both located inside the ionic core of the aggregate, and the d_1 values, as a function of the degree of neutralization, x.

at 333−360 K. This replacement has been considered an indication of a microphase separation of ionic aggregates from the matrix into a separate domain with its own T_g, in addition to the T_g of the polyethylene matrix.

In the present ESR studies, the splitting of outer peaks of 7DSE and 10DND for $x = 0.6$, 0.8, and 0.9 supports the model of two dynamical states of the amorphous region.

(c) Comparison of ESR and SAXS Results: Polarity vs Electron Density. The variations of the polarity indices for 5DSA and 7DSA (derived from ESR data) and of the electron density of the ionic core, d_1, of the aggregate (derived from SAXS) as a function of x are presented in Figure 8. The dependence of d_1 on x is qualitatively similar to that of ΔA_0 of the probes, though slightly closer to the behavior of 7DSA than of 5DSA. We note that d_1 is an average value throughout the ionic core of the aggregate for each x, whereas ΔA_0 reflects the local polarity in the ionic core reported by the probe. Hence, the above result means that the probe site for 7DSA roughly reflects the average electron density of the ionic core of the aggregate. The spin probe ESR technique has the advantage of determining the local environment inside ionic aggregates, and different spin probes reflect different and specific regions.

We have also applied the spin-probe ESR technique to the Mg and Zn salts of EMAA ionomers. For the Mg salts, the $2A'_{zz}$ values at 293 K were sensitive to both the probe site and the degree of neutralization x; for $x = 0.6$, for example, the $2A'_{zz}$ values at 293 K were 64.5, 62.1, 60.6, 60.1, and 60.2 G for 5DSA, 7DSA, 10DSA, 7DSE, and 10DND, respectively; the $2A'_{zz}$ value of 5DSA increased from 62.9 G for $x = 0.2$ to 65.3 G for $x = 0.9$. These results are similar to those for the Na salts of EMAA, described above. For the Zn salts, however, the $2A'_{zz}$ values of the probes at 293 K were not sensitive to the x value; the $2A'_{zz}$ value of 5DSA was in the range between 63.2 and 63.9 G without any clear dependence on x. These results might be associated with the small size of the ionic aggregate in the Zn salts, but it is more likely that they reflect the covalent nature of COO−Zn coordination bonds. The spin probe ESR technique is very useful for the study of local environments in alkali-metal and alkaline-earth-metal salts of ionomers but not for the transition-metal salts. This conclusion is in full agreement with recent results on ionomers neutralized by Na^+ and Cu^{2+} ions.[35]

Conclusions

The local structure in and near the ionic aggregates in EMAA-xNa ionomers was investigated by spin-probe ESR and SAXS. The ESR studies revealed that the five spin probes used are position-selective and provide local information on different regions in the ionomers. Three hydrophilic doxylstearic acid probes, nDSA, are anchored to the ionic aggregates: two (5DSA and 7DSA) are located in the ionic core, and one (10DSA) is in the hydrocarbon shell; the two hydrophobic probes (7DSE and 10DND) report on the amorphous region. The variation of the polarity indices (ΔA_0) of these position-selective probes as a function of the degree of neutralization indicated the presence of an ion-depleted zone (hydrocarbon shell) surrounding the ionic core and also the presence of a small amount of isolated ionic groups in the amorphous regions.

The structural features deduced by ESR were in support of the SAXS profile analysis based on a depleted-zone core−shell structure of the aggregate. The SAXS studies provided additional information on the geometrical shape and size of the aggregate and the number of ionic groups in each aggregate. Thus, microstructural insights into the ionic aggregate from both approaches, polarity from ESR and electron density from SAXS, are consistent and complementary.

Acknowledgment. In the US this study was supported by the Polymers Program of the National Science Foundation. We thank Mr. Yoshikazu Kutsuwa and Mr. Tatsuya Watanabe of Technical Center, Du Pont-Mitsui Polychemicals Co. Ltd., Chiba, Japan, and Dr. Eisaku Hirasawa of Fujimori Kogyo Co. Ltd., for kindly donating the ionomer samples and for encouragement and very helpful discussions; and Prof. Hiroyuki Tagawa of Nihon University Junior College and Dr. Yoshio Muroga of Nagoya University for help with the SAXS measurements. We also thank Prof. Takashi Kawamura of Gifu University, Japan, for the use of the ESR spectrometer and the Photon Factory Program Advisory Committee, the National Laboratory for High Energy Physics, Tsukuba, Japan, for their approval of our SAXS measurements (proposal 94G125). We thank Ewa Szajdzinska-Pietek of Technical University of Lodz, Poland, for critical reading of the manuscript and useful comments.

References and Notes

(1) *Ionomers: Characterization, Theory, and Applications*; Schlick, S., Ed.; CRC Press: Boca Raton, FL, 1996.
(2) *Ionomers: Synthesis, Structure, Properties and Applications*; Tant, M. R., Mauritz, K. A., Wilkes, G. L., Eds.; Blackie Academic and Professional: London, 1997.
(3) Rees, R. W.; Vaughan, D. J. *Polym. Prepr.* (*Am. Chem. Soc., Div. Polym. Chem.*) **1965**, *6*, 287.
(4) Longworth, R.; Vaughan, D. J. *Nature* (*London*) **1968**, *218*, 85.
(5) Register, R. A.; Cooper, S. L. *Macromolecules* **1990**, *23*, 318.
(6) (a) Laurer, J. H.; Winey, K. I. *Macromolecules* **1998**, *31*, 9106. (b) Winey, K. I.; Laurer, J. H.; Krikmeyer, B. P. *Macromolecules* **2000**, *33*, 507.
(7) (a) McLean, R. S.; Doyle, M.; Sauer, B. B. *Macromolecules* **2000**, *33*, 6541. (b) Sauer, B. B.; McLean, R. S. *Macromolecules* **2000**, *33*, 7939.
(8) Yarusso, D. J.; Cooper, S. L. *Polymer* **1985**, *26*, 371.
(9) Eisenberg, A.; Hird, B.; Moore, R. B. *Macromolecules* **1990**, *23*, 4098.
(10) Vanhoorne, P.; Jérôme, R.; Teyssié, P.; Lauprêtre, F. *Macromolecules* **1994**, *27*, 2548.
(11) Pineri, M.; Meyer, C.; Levelut, A.-M.; Lambert, M. *J. Polym. Sci., Polym. Phys. Ed.* **1974**, *12*, 115.

(12) Grady, B. P.; Cooper, S. L. In ref 2, pp 48−50 and references therein.
(13) Szajdzinska-Pietek, E.; Schlick, S. In ref 1; Chapter 7, pp 135−163.
(14) Martini, G.; Ottaviani, M. F.; Ristori, S.; Visca, M. *J. Colloid Interface Sci.* **1989**, *128*, 76.
(15) Szajdzinska-Pietek, E.; Schlick, S.; Plonka, A. *Langmuir* **1994**, *10*, 1101.
(16) Szajdzinska-Pietek, E.; Schlick, S.; Plonka, A. *Langmuir* **1994**, *10*, 2188.
(17) Szajdzinska-Pietek, E.; Pilar, J.; Schlick, S. *J. Phys. Chem.* **1995**, *99*, 313.
(18) Tsagaropoulos, G.; Kim, J.-S.; Eisenberg, A. *Macromolecules* **1996**, *29*, 2222.
(19) Kutsumizu, S.; Hara, H.; Schlick, S. *Macromolecules* **1997**, *30*, 2320.
(20) Kutsumizu, S.; Schlick, S. *Macromolecules* **1997**, *30*, 2329.
(21) Szajdzinska-Pietek, E.; Pillars, T. S.; Schlick, S.; Plonka, A. *Macromolecules* **1998**, *31*, 4586.
(22) Schädler, V.; Franck, A.; Wiesner, U.; Spiess, H. W. *Macromolecules* **1997**, *30*, 3832.
(23) Pannier, M.; Schädler, V.; Schöps, M.; Wiesner, U.; Jeschke, G.; Spiess, H. W. *Macromolecules* **2000**, *33*, 7812.
(24) Gebel, G.; Lambard, J. *Macromolecules* **1997**, *30*, 7914.
(25) Loppinet, B.; Gebel, G.; Williams, C. E. *J. Phys. Chem. B* **1997**, *101*, 1884.
(26) Gebel, G.; Loppinet, B.; Hara, H.; Hirasawa, E. *J. Phys. Chem. B* **1997**, *101*, 3980.
(27) Yano, S.; Tadano, K.; Nagao, N.; Kutsumizu, S.; Tachino, H.; Hirasawa, E. *Macromolecules* **1992**, *25*, 7168.
(28) Hirasawa, E.; Yamamoto, Y.; Tadano, K.; Yano, S. *J. Appl. Polym. Sci.* **1991**, *42*, 351.
(29) Kutsumizu, S.; Nagao, N.; Tadano, K.; Tachino, H.; Hirasawa, E.; Yano, S. *Macromolecules* **1992**, *25*, 6829.
(30) (a) Ueki, T.; Hiragi, Y.; Kataoka, M.; Inoko, Y.; Amemiya, Y.; Izumi, Y.; Tagawa, H.; Muroga, Y. *Biophys. Chem.* **1985**, *23*, 115. (b) Kutsumizu, S.; Tagawa, H.; Muroga, Y.; Yano, S. *Macromolecules* **2000**, *33*, 3818.
(31) MacKnight, W. J.; Taggart, W. P.; Stein, R. S. *J. Polym. Sci., Polym. Symp.* **1974**, *45*, 113.
(32) Speakman, J. C.; Mills, H. H. *J. Chem. Soc.* **1961**, 1164.
(33) Griffith, O. H.; Jost, P. C. In *Spin Labeling. Theory and Applications*; Berliner, L. J., Ed.; Academic Press: New York, 1976; pp 453−523.
(34) Yano, S.; Nagao, N.; Hattori, M.; Hirasawa, E.; Tadano, K. *Macromolecules* **1992**, *25*, 368.
(35) Kruczala, K.; Schlick, S. *J. Phys. Chem. B* **1999**, *103*, 1934.

MA012132Y